

One Dimensional Pollutant Transport Model

by

B.Senthilkumar

Thesis submitted to the Faculty of the
Virginia Polytechnic Institute and State University
in partial fulfillment of the requirements for the degree of
Master of Science
in
Civil Engineering

APPROVED:

T.Kuppusamy, Chairman

G.W.Clough

J.C.Parker

May, 1986

Blacksburg, Virginia

One Dimensional Pollutant Transport Model

by

B.Senthilkumar

T.Kuppusamy, Chairman

Civil Engineering

(ABSTRACT)

This thesis presents the development of a numerical model for one-dimensional pollutant transport in a porous medium. A computer program POLUTE1D has been developed. The numerical model is based on the flow and mass transport equations and the finite element method has been used for its formulation. The problem involves unsaturated flow and convective dispersive transport of a contaminant species. A literature survey on the evaluation of the dispersion coefficient is included. A waste disposal dump site is analysed as a one-dimensional problem by using this model. The effect of the liner thickness, the liner permeability, the ponding head and the initial condition of the porous domain on the spread of the contaminant is studied. Conclusions are presented based on a parametric study.

Acknowledgements

I owe a debt of gratitude to many people for their support and assistance in the completion of this thesis. First I would like to express my thanks and gratitude to my uncle and aunt, Ramesh and Pathma Ramesvara, for all their support, both financial and emotional. They provided me with the opportunity to continue my education, that I may never have been able to pursue on my own.

I am also indebted to my major professor, Dr.T.Kuppusamy, for all the guidance he provided throughout this work. Thanks must be extended to Dr.J.C.Parker and Dr.G.W.Clough for reviewing this thesis and making valuable suggestions.

Heartfelt thanks are extended to Jopan Sheng for his assistance with the programming, his willingness to listen as I "brainstormed", and for being a good friend.

Finally, I owe a special debt of gratitude to my parents, for their support and encouragement, their understanding, their sacrifices and their help throughout my career.

Table of Contents

Chapter 1	1
Introduction	1
Chapter 2	3
Basic Concepts in Pollutant Transport Through a Porous Medium	3
2.1 General	3
2.2 Flow Equations	4
2.3 θ - h Relationship	7
2.4 Hydraulic Conductivity	13
2.5 Mass Transport Equation	14
2.6 Dispersion Coefficient	16
Chapter 3	21
Finite Element Formulation	21
3.1 General	21
3.2 Governing Equations	22
3.3 Finite Element Formulation	22

3.4 Solution in time	27
3.5 Non Linear Technique	29
3.5.1 Picard's method	29
3.5.2 Newton - Raphson method	29
3.6 POLUTE1D	32
Chapter 4	34
Parameteric Study	34
4.1 Introduction	34
4.2 Parameters	36
4.3 The effect of liner thickness	39
4.4 The effect of liner permeability	42
4.5 The effect of liner dispersivity	42
4.6 The effect of ponding depth	45
4.7 The effect of initial condition	45
Chapter 5	48
Summary and Conclusions	48
Bibliography	50
Vita	52

List of Illustrations

Figure 1. One Dimensional Problem	5
Figure 2. Apparatus to obtain θ - h relationship	8
Figure 3. Typical θ - h curve	9
Figure 4. Effects of α and n	12
Figure 5. Unsaturated hydraulic conductivity	15
Figure 6. Picard's method	30
Figure 7. Newton - Raphson method	31
Figure 8. Modified Picard's method	33
Figure 9. One-dimensional problem	35
Figure 10. θ - h relationship for sandy clay loam and clay used in the example.	38
Figure 11. Pollutant spread with time in the porous medium	40
Figure 12. Effect of liner thickness on pollutant transport	41
Figure 13. Effect of liner permeability at a point	43
Figure 14. Effect of liner dispersivity at a point	44
Figure 15. Effect of ponding depth on pollutant transport	46
Figure 16. Effect of the initial condition	47

List of Tables

Table 1. Parameter values for Van Genuchten model determined from transient one-step outflow experiments (Kool et al., 1985)	11
Table 2. Summary of dispersion equations	19
Table 3. Diffusion coefficients of solutes (Ross 1977)	20
Table 4. Time integration methods	28
Table 5. Representative values for sandy clay loam and clay (Kool et al., 1986)	37

Chapter 1

Introduction

During the past decade, hazardous waste disposal has become one of the major environmental problems facing many nations. The pollution problem is a slow-acting, non-visible phenomenon, which can involve a gradual contamination of the good water as it flows from the hazardous waste site. It takes years for people to find out whether they or their children are victims of chemical poisoning.

US industries generate about 300 million tons of toxic waste per year. These chemicals have in too many cases been dumped all over the US in the mistaken belief that the toxicity will be lost with time before it seeps into ground water, and many of these dumpsites are leaking and contaminating the ground water. It is a serious challenge for the Environmental Protection Agency (EPA) to remedy this misguided practice with too little resources in too short a time. However, there is no other alternative at the moment than to put these waste materials in landfills which are going to leak some day.

Now that all are aware of this problem, it has given rise to the situation where every community says, "No dumpsites in my backyard". To alleviate the fears of these communities, the dumpsites should be located in remote areas and they should have a good liner of sufficient thickness to prevent seepage through the layers of soil and rock into ground water supplies.

In this report, a finite element mathematical model is presented, which may be used to predict the liner thickness and liner permeability with a reasonable accuracy. Also by using this model, the spread of the contaminant in a landfill could be determined.

Chapter Two explains the basic concepts involved in modeling pollutant transport models. This chapter contains the flow and mass transport equations, the constitutive laws, the volumetric water content - capillary pressure relationship and details about the dispersion coefficient.

The finite element formulation of the model is given in Chapter Three. Chapter Four is a parametric study of the effects due to the changes in liner thickness and permeability, ponding pressure and initial condition on pollutant concentration in the porous domain.

Chapter 2

Basic Concepts in Pollutant Transport Through a Porous Medium

2.1 General

The study of pollutant transport is very costly if it relies entirely on field investigation. For this reason, investigators often turn to numerical models as tools to predict pollutant transport in a porous medium. Although such approaches can be powerful, it should be born in mind, that the numerical prediction will be only as good as the hydrologic setting and available data which are input into the model.

A dumpsite which is extensive may be analysed as a one-dimensional problem. That is, if it has a large longitudinal and lateral dimension, the problem is idealized to a one-dimensional case, where the pollutant will flow only in the vertical direction (Figure 1 on page 5). In this

case there are two different phenomena taking place: the flow of water through the unsaturated medium and the dispersion of the pollutant concentration.

2.2 Flow Equations

The constitutive law for the flow problem is Darcy's Law.

$$q = -k \frac{\partial H}{\partial Z} \quad [2.1]$$

where q = Hydraulic flux density

k = Hydraulic conductivity

H = Hydraulic head

Z = Depth

The velocity in eqn (2.1) is in the Z direction. Since the velocity decreases with the gradient, a negative sign occurs in eqn (2.1).

For seepage flow in a porous medium, Darcy's Law is valid if the flow occurs with a very low value (nearly equal to zero) of Reynold's number Re or with $Re < 0$. When the particle size is less than 1 mm, the latter may be assumed to occur. Hence, if the porous medium is clayey, silty, or silty-fine sands, the application of Darcy's Law is justified.

The equations used in this presentation are based on the assumptions that the medium is rigid, the fluid is homogeneous and incompressible, the flow is continuous and irrotational and the capillary, air convection and inertia effects are negligible.

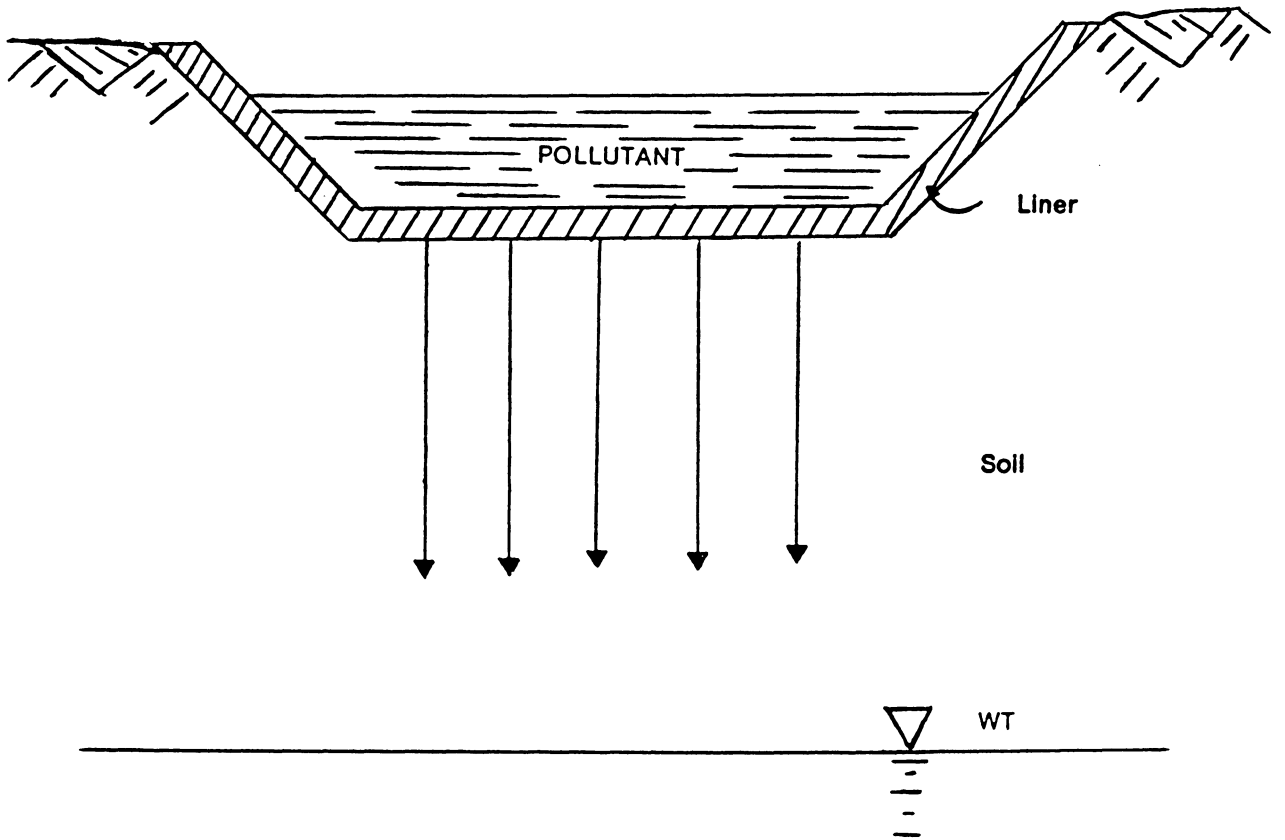


Figure 1. One Dimensional Problem

The one-dimensional vertical flow equation for an incompressible fluid in a rigid porous medium may be obtained from a solution to Richard's equation (Huyakorn et al., 1983) which may be written as

$$C_h \frac{\partial h}{\partial t} = \frac{\partial}{\partial Z} \left[k \left(\frac{\partial h}{\partial Z} - 1 \right) \right] \quad [2.2]$$

where h = Capillary pressure head

t = Time

Z = Depth taken positive downwards

k = Unsaturated hydraulic conductivity

$$= k_r k_{sat}$$

k_r = Relative conductivity ratio

k_{sat} = Saturated hydraulic conductivity

$$C_h = \frac{d\theta}{dh}$$

= Water capacity

θ = Volumetric water content

$$= \frac{\text{Volume of water}}{\text{Total volume}}$$

To obtain the parameters k and C_h , one has to determine water content θ vs pressure h relationship of the porous medium.

2.3 θ - h Relationship

An apparatus to determine the θ - h curve is shown in Figure 2 on page 8. The porous sample is initially saturated with water. The volume of water needed to saturate the sample can be calculated. Air is pumped in under pressure from the top of the sample, while the water level in the outer tube is kept constant. When the soil water gets stabilized in the sample, the outflow from the sample can be measured. This outflow is the water displaced by air in the porous sample. Hence the volume of water now in the porous medium can be computed. This leads us to the present volumetric water content in the porous sample. determined from the observed outflow. Hence for the known applied pressure, the volumetric water content of the sample can be obtained. Repeating the experiment for varying pressures, a set of points may be obtained for the plot of the θ - h curve.

Figure 3 on page 9 shows the typical relationship between θ and h. In this figure θ_s is the saturated water content and θ_r is the residual water content. θ_s can be determined experimentally. The residual water content θ_r is defined as the water content at which the gradient $\frac{d\theta}{dh}$ in the $\theta - h$ curve becomes zero at a very large h. However, in Figure 3 on page 9 it should be noted that the slope $\frac{d\theta}{dh}$ becomes zero near θ_r , as well as near the saturation point θ_s . This relationship also indicates the pore size distribution of the porous medium. An analogy for this characteristic may be made by considering a bundle of capillary tubes of various radii. The capillary rise in a tube relative to the free surface and hence the fluid pressure head is inversely proportional to its radius, due to the surface tension forces acting on the tube. Therefore, if the soil is very porous, the pressure-head will be low and vice versa.

This curve will have a hysteresis, if wetting and drying experiments are conducted in the porous medium. There are models available describing this phenomenon. However, for our purpose, the hysteresis will be disregarded and the drying curve will be assumed to represent the $\theta - h$ curve.

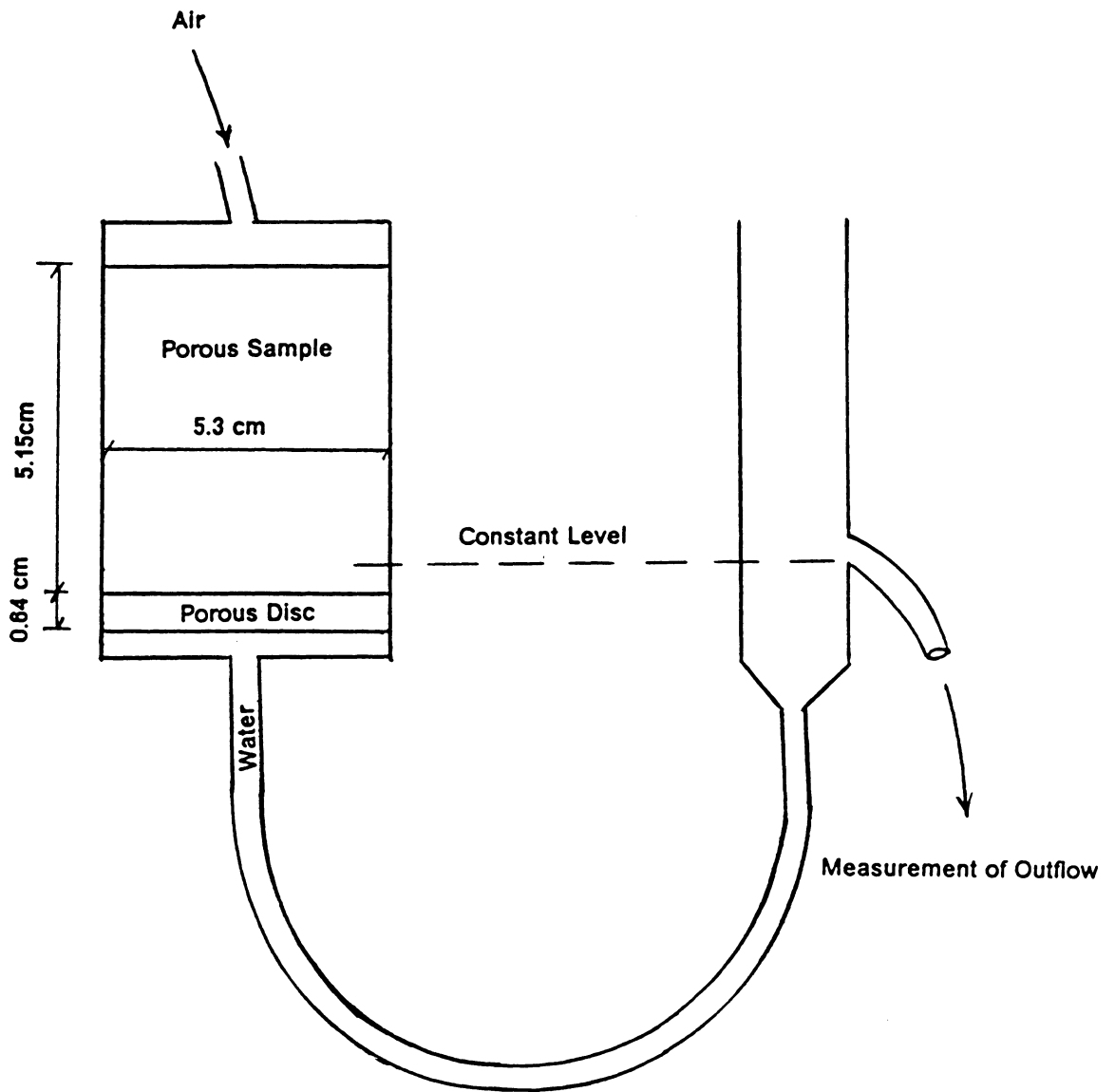


Figure 2. Apparatus to obtain θ - h relationship

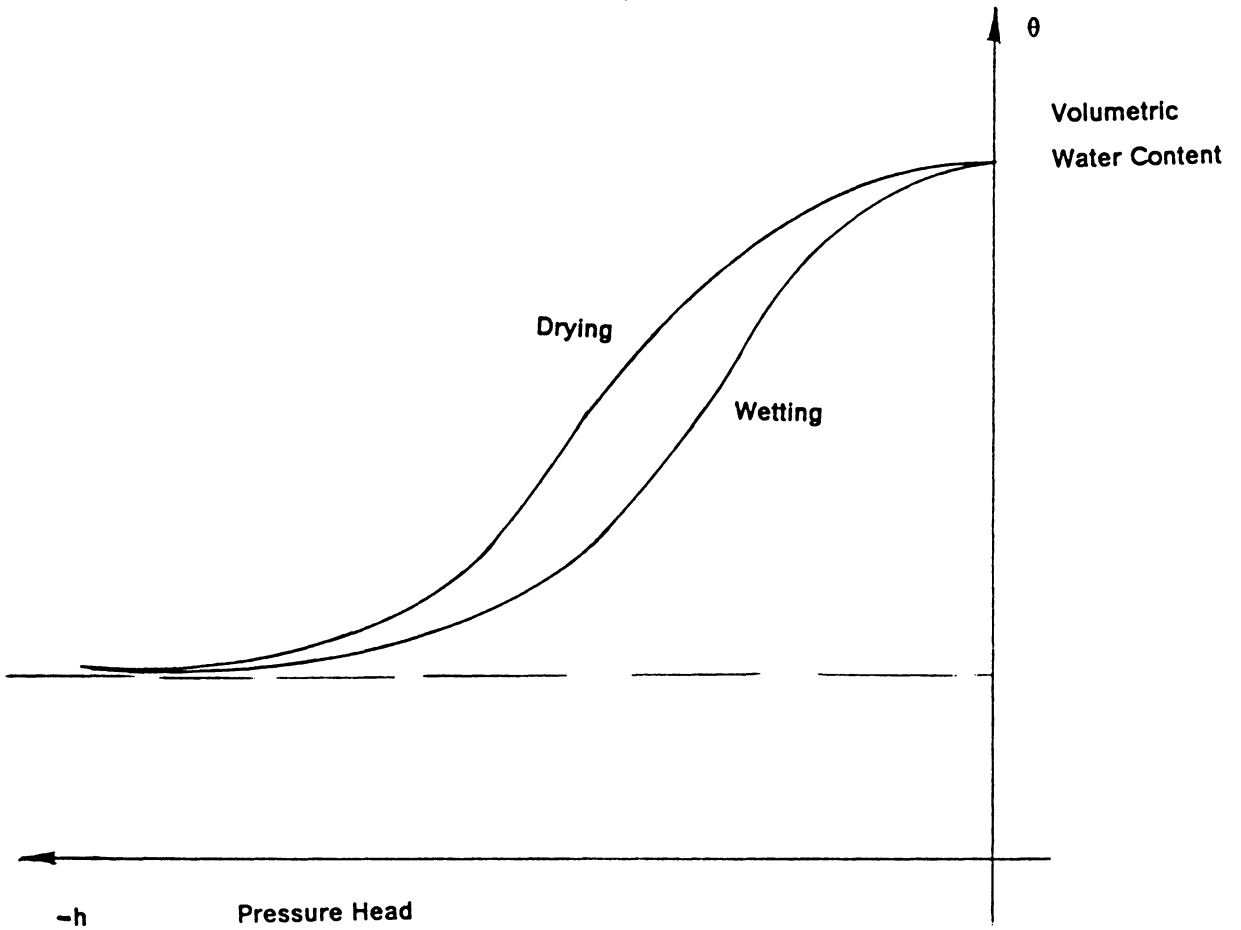


Figure 3. Typical θ - h curve

Van Genuchten (1978) describes the $\theta - h$ relationship with the empirical form

$$\theta = \theta_r + \frac{\theta_s - \theta_r}{[1 + |\alpha h|^n]^{(1 - \frac{1}{n})}} \quad \text{for } h < 0 \quad [2.3]$$

$$\theta = \theta_s \quad \text{for } h \geq 0$$

where θ_r , α and n are the empirical parameters which are determined by fitting the best curve, for the experimental data. Typical values of α and n for few soils are given in Table 1 on page 11.

The S_e vs h curve is shown in Figure 4 on page 12. S_e has a value of 1.0 when h is zero. While n is constant, if α is increased from 1 to 5, the curve shifts towards the vertical axis. If α is kept constant and n is increased from 1 to 2, the slope of the curve becomes shallower. α and n are simply curve-fitting parameters.

The water capacity is the slope of the $\theta - h$ curve. Differentiating eqn (2.3) with respect to h , the water capacity is obtained as

$$C_h = \frac{d\theta}{dh} \quad [2.4]$$

$$= \frac{-\alpha n(\theta_s - \theta_r)}{1 - m} S_e^{\frac{1}{m}} \left(1 - S_e^{\frac{1}{m}}\right)^m$$

Textural class	Particle size distribution			Bulk density (lb/cu.ft)	Parameter Values				
	sand	silt	clay		α ft^{-1}	n	θ_r	θ_s	k_s $ft\ day^{-1}$
sandy loam	61	24	15	1550	0.375	1.301	0.110	0.355	0.2
silt loam	28	56	15	1570	1.44	1.461	0.173	0.388	4.3
sandy clay loam	56	18	26	1530	0.71	1.225	0.199	0.402	0.3
clay	21	31	48	1110	0.15	1.319	0.127	0.589	0.0006

Table 1. Parameter values for Van Genuchten model determined from transient one-step outflow experiments (Kool et al., 1985)

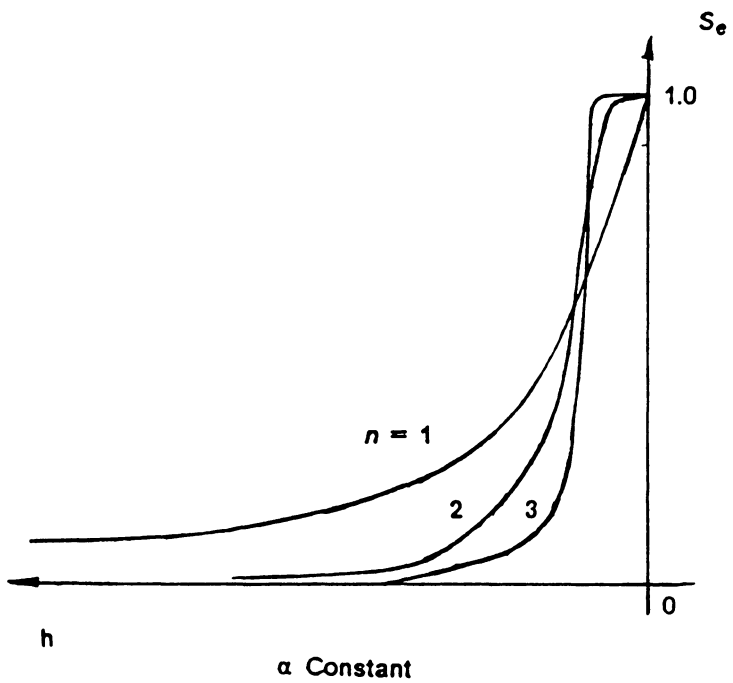
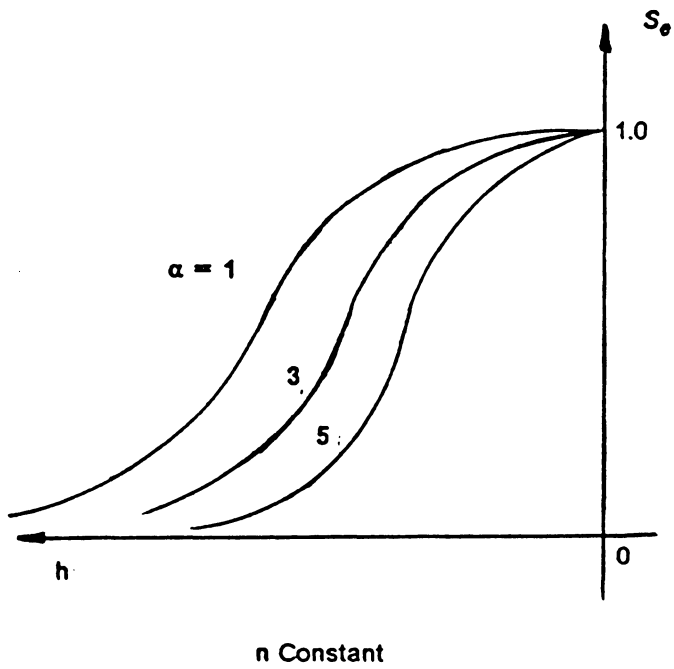


Figure 4. Effects of α and n

2.4 Hydraulic Conductivity

The relative hydraulic conductivity (k_r) is the ratio between the unsaturated conductivity and the saturated conductivity (k_s) of a porous medium. Using the same analogy as before, consider the soil mass as a bundle of capillary tubes. Since k is proportional to r^2 where r is the capillary radius, it is possible to relate $\theta(h)$ to pore-size distribution and to predict $k(\theta)$. There are a number of models available depending on these analyses. Mualem (1976) derives the following equation for relative hydraulic conductivity.

$$k_r = S_e^{\frac{1}{2}} \left[\frac{\int_0^{S_e} \frac{1}{h}(x) dx}{\int_0^1 \frac{1}{h}(x) dx} \right]^2 \quad [2.5]$$

where h is the pressure head, given as a function of the effective saturation. The first term $S_e^{1/2}$ results because of the assumptions made about the connectivity of the capillary tubes.

From eqn (2.4) Van Genuchten (1978) derives his expression for relative hydraulic conductivity as follows:

$$k_r(S_e) = S_e^{\frac{1}{2}} \left[1 - \left(1 - S_e^{\frac{1}{m}} \right)^m \right]^2 \quad \left(m = 1 - \frac{1}{n} \right) \quad [2.6]$$

$$(0 < m < 1)$$

Substituting eqn (2.3) in eqn (2.5), the relative hydraulic conductivity can be written in terms of pressure head as

$$k_r(h) = \frac{\left[1 - (\alpha h)^{n-1} \{ 1 + (\alpha h)^n \}^{-m} \right]^2}{\left[1 + (\alpha h)^n \right]^{\frac{m}{2}}} \quad [2.7]$$

The relationship of k and h in eqn (2.6) could be graphically displayed as in Figure 5 on page 15.

2.5 Mass Transport Equation

The one-dimensional mass-transport equation may be written as (Huyakorn et al., 1983)

$$R \frac{\partial c}{\partial t} = D \frac{\partial^2 c}{\partial Z^2} - v \frac{\partial c}{\partial Z} + \bar{K}c + \bar{Q} \quad [2.8]$$

where c = Concentration

D = Dispersion coefficient

v = Mean pore water velocity = $\frac{q}{\theta}$

t = Time

Z = Depth

R = Retardation coefficient

\bar{K} = First-order decay coefficient

\bar{Q} = Zero-order source or sink

The coefficient \bar{K} is used in a situation where the material undergoes first-order decay. For the occurrence of mass transport with adsorption, the retardation coefficient R is applied.

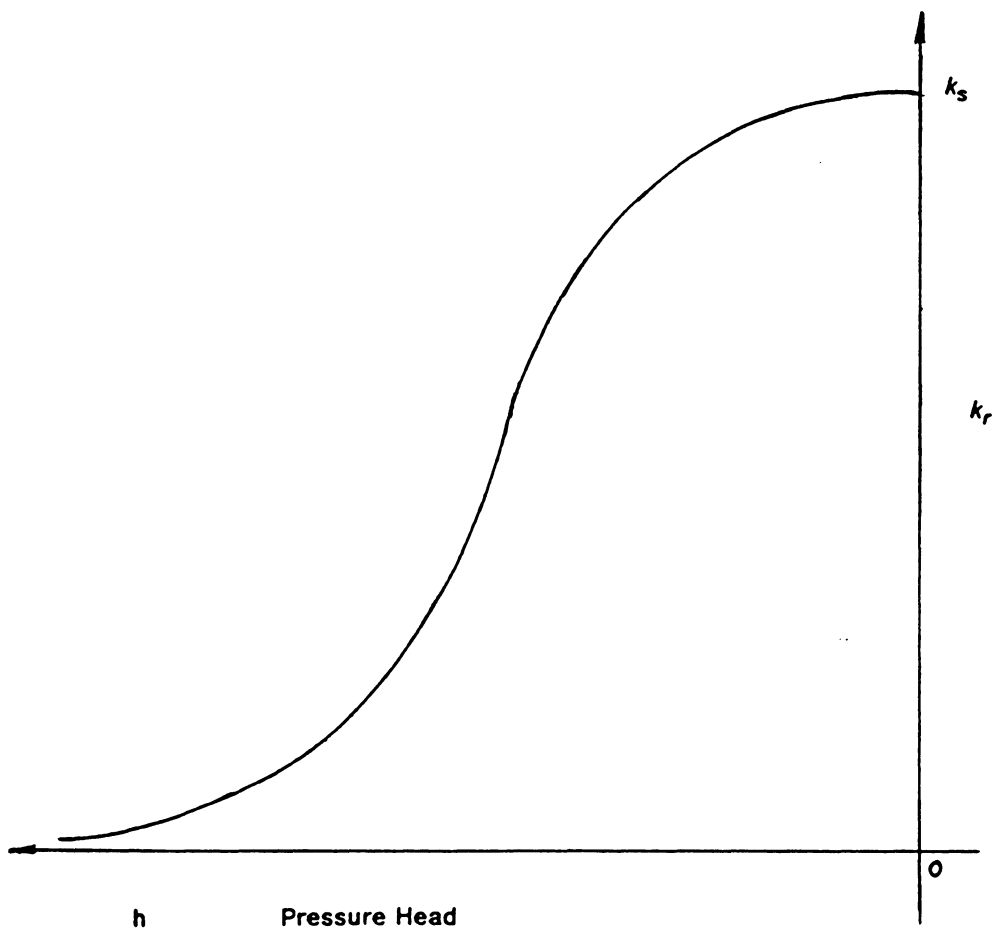


Figure 5. Unsaturated hydraulic conductivity

2.6 Dispersion Coefficient

The dispersion coefficient D of a material is due to its mechanical or convective dispersion and molecular diffusion. Convective dispersion is the movement of pollutants associated with bulk flow of the liquid phase. This is the most important mechanism in the transport of pollutant. Hence, convection depends largely on ground water movement which in turn relies on the pressure head, the permeability and the porosity.

If the contaminant is mixed with water due to the random movement of the molecules, it is termed 'molecular diffusion'. As an example, if one adds alcohol to a glass of water and lets the mixture sit still, the spreading of the alcohol in the water is due to molecular diffusion. When a rod is inserted in the glass and stirred, significant mixing will occur. This is due to the convective dispersion and depends on the direction and magnitude of the velocity of the fluid.

Taylor (1953) considers D as proportional to v^2 where v is the average pore-fluid velocity. Bear and Todd (1960) introduces $D = a_1 v$ where a_1 is some characteristic medium length.

In Saffman's (1960) model the dispersion coefficient is stated as

$$\frac{D}{D_o} = T_m + \frac{P^2}{15} \quad \text{for } P < 1$$

$$\frac{D}{D_o} = T_m + \frac{P}{6} \left[\ln\left(\frac{3P}{2}\right) - \frac{17}{12} - \frac{P}{8} \left(\frac{a}{\ell}\right)^2 \right] + \frac{4}{9} \quad \text{for } 1 < P < 8 \left(\frac{\ell}{a}\right)^2$$

where D_o = Diffusion coefficient of solute

D_m = Diffusion coefficient of solute in macropores

v = Mean fluid velocity

$T_m = \frac{D_m}{D_o}$ = Tortuosity of macropores

= $\frac{2}{3}$ in Saffmans model

$P = \frac{vd}{D_o}$ = Peclet number

d = Particle diameter

ℓ = Pore length

a = Pore radius

Ross (1977) describes the dispersion coefficient D as

$$\frac{D}{D_o} = \frac{D_m}{D_o} + k_1 \left(\frac{vd}{D_o} \right)^n$$

$$\frac{D}{D_o} = T_m + k_1 P^n$$

where k_1, n = Empirical constants which depends on the characteristics of the porous media

Ross (1977) reports values for k_1 between 0.16 and 7.9 and for n between 1.0 and 1.56. However, Brigham et al.,(1961) has reported values as high as 53 for k_1 .

The viscosity ratio of fluids and the homogeneity of the porous material affects the values of k_1 and n (Brigham et al., 1961). Also these constants depend on the values of D_o (Ross 1977).

B.S.Ghuman et al., (1980) formulates:

$$D_a = mv_p^n$$

where D_a = Apparent dispersion coefficient

v_p = Pore water velocity

m, n = Constants characterizing the porous medium

Table 2 on page 19 summarizes the various equations describing the dispersion coefficient. Considering all the equations in Table 2 on page 19, a more generalized equation for the dispersion coefficient may be written as

$$\frac{D}{D_o} = a\theta^b + k_1P^n \quad [2.9]$$

where D = Dispersion coefficient of solute

D_o = Diffusion coefficient of solute

$$P = \frac{v\ell}{D_o} = \text{Peclet number}$$

a, b, k_1, n = Empirical constants

v = Mean fluid velocity in pore space

ℓ = 'Characteristic length' of porous medium

For our study eqn (2.9) is used to calculate D in the mass transport eqn (2.8). Table 3 on page 20 gives the values for the diffusion coefficient D_o . The values used for a, b, k_1 and n are 0.67, 1, 0.5 and 1 respectively as per Ross (1977). The dispersivity ϵ , of the soil is defined as $k_1\ell$, using the above parameters.

	Dispersion Equations
Taylor (1953)	$D \propto v^2$
Bear & Todd (1960)	$D = a_1 v$
Saffman (1960)	$\frac{D}{D_0} = T_m + \frac{P^2}{15} \quad \text{for } P < 1$ $\frac{D}{D_0} = T_m + \frac{P}{6} \left[\ln\left(\frac{3P}{2}\right) - \frac{17}{12} - \frac{P}{8} \left(\frac{a}{l}\right)^2 \right]$ $+ \frac{4}{9} \quad \text{for } 1 << P << 8 \left(\frac{l}{a}\right)^2$
B.S.Ghuman et al., (1980)	$D_* = m v^n$
Ross (1977)	$\frac{D}{D_0} = T_m + k_1 P^n$

Table 2. Summary of dispersion equations

	Diffusion Coefficients D_0 (ft ² day ⁻¹)
Gases	10
Inorganic solute ions	10 ⁻³
Organic molecules	10 ⁻⁵

Table 3. Diffusion coefficients of solutes (Ross 1977)

Chapter 3

Finite Element Formulation

3.1 General

The finite element technique is one of the versatile and favoured simulation methods available for the study of pollutant transport in a porous medium. Since soil in its natural condition is highly inhomogeneous, irregular, and nonlinear, the finite element method is ideally suited to account for them. In this chapter, the finite element formulation of the governing equations of unsaturated flow and pollutant transport, will be described.

Rowe (1984) used closed form solution for his one dimensional pollutant transport model with constant dispersion coefficient D . The finite difference technique has been widely used for solving mass transport problems (Huyakorn et al., 1983). A one dimensional finite element model was developed by Guymon (1970), for transport problems assuming steady state flow. Also there are several two dimensional finite element codes for mass transport problems

(Guymon., 1970, Huyakorn et al., 1983). Essentially in all these programs, the mass transport equations are solved assuming the velocity field. In this study the flow equation is used to get the velocity and couple it with the mass transport equation to get the concentration spread. Also the Van Genuchten model for unsaturated flow and a varying dispersion coefficient with velocity and water content are used.

3.2 Governing Equations

The numerical model is to be based upon the governing differential equations for the flow and mass transport given below.

$$C_h \frac{\partial h}{\partial t} = \frac{\partial}{\partial Z} \left[k \left(\frac{\partial h}{\partial Z} - 1 \right) \right] \quad [3.1]$$

$$R \frac{\partial c}{\partial t} = D \frac{\partial^2 c}{\partial Z^2} - v \frac{\partial c}{\partial Z} + \bar{K} c + \bar{Q} \quad [3.2]$$

3.3 Finite Element Formulation

The main procedures used for formulating finite element equations are the variational and residual methods. The functional associated with the flow eqn (3.1) is given by

$$\lambda = \int \left[\frac{1}{2} k \left(\frac{\partial h}{\partial Z} \right)^2 + C_h h \frac{\partial h}{\partial t} \right] dZ - \bar{q} h \Big|_{\text{flux boundary}} \quad [3.3]$$

where \bar{q} is the fluid flux and for no-flow condition, this becomes zero.

For a two-noded, one-dimensional element, the shape functions are assumed linear and given as below.

$$h = [N] \{q_h\} \quad [3.4]$$

$$h = \left[\frac{1}{2}(1-L) \quad \frac{1}{2}(1+L) \right] \begin{Bmatrix} h_1 \\ h_2 \end{Bmatrix}$$

where L is the local coordinate and $\{q_h\} = \begin{Bmatrix} h_1 \\ h_2 \end{Bmatrix}$

Differentiating eqn (3.4) with respect to Z and t we have,

$$\frac{\partial h}{\partial Z} = \frac{1}{\ell} \begin{bmatrix} -1 & -1 \end{bmatrix} \begin{Bmatrix} h_1 \\ h_2 \end{Bmatrix}$$

$$\text{ie., } \frac{\partial h}{\partial Z} = [B] \{q_h\} \quad [3.5]$$

$$\begin{aligned} \text{and } \frac{\partial h}{\partial t} &= \frac{\partial}{\partial t} \left[\frac{1}{2}(1-L)h_1 + \frac{1}{2}(1+L)h_2 \right] \\ &= [N] \begin{Bmatrix} \frac{\partial h_1}{\partial t} \\ \frac{\partial h_2}{\partial t} \end{Bmatrix} \end{aligned}$$

which may be written as,

$$\frac{\partial h}{\partial t} = [N] \{q_h\} \quad [3.6]$$

Substituting eqns (3.5) and (3.6) into eqn (3.3) and taking variations will lead to the element equation

$$[K] \{q_h\} + [K_t] \{\dot{q}_h\} = \{Q_h\} \quad [3.7]$$

$$\text{where } [K] = \int_{Z_1}^{Z_2} [B]^T k [B] dZ$$

$$= \frac{k}{\ell} \begin{bmatrix} 1 & -1 \\ -1 & 1 \end{bmatrix}$$

$$[K_T] = \int_{Z_1}^{Z_2} C_h [N]^T [N] dZ$$

$$= \frac{C_h \ell}{3} \begin{bmatrix} 1 & \frac{1}{2} \\ \frac{1}{2} & 1 \end{bmatrix}$$

$$Q_h = \bar{q} \text{ at the flux boundary}$$

The element equations are assembled to obtain the global equations and solved for the nodal values of h . Substituting this into eqn (3.5) the fluid velocity v for each element can be obtained.

For the mass transport problem, the same element with linear shape functions given in eqn (3.4) is again used.

$$C = \left[\frac{1}{2}(1-L) \quad \frac{1}{2}(1+L) \right] \begin{Bmatrix} c_1 \\ c_2 \end{Bmatrix}$$

$$C = [N_1 \quad N_2] \begin{Bmatrix} c_1 \\ c_2 \end{Bmatrix}$$

$$C = \sum N_j C_j \quad [3.8]$$

The element equations are derived by the Galerkin's Method of Weighted Residual. Weighting the residual with respect to N_i , we have

$$\int_{z_1}^{z_2} \left[\frac{\partial}{\partial Z} \left(D \frac{\partial c}{\partial Z} \right) - v \frac{\partial c}{\partial Z} - A \frac{\partial c}{\partial t} - \bar{K}c + \bar{Q} \right] N_i dZ = 0 \quad [3.9]$$

Substitution of eqn (3.8) into eqn (3.9) will yield

$$\int_{z_1}^{z_2} \left[\frac{\partial}{\partial Z} \left(D \frac{\partial}{\partial Z} (N_j C_j) \right) - v \frac{\partial}{\partial Z} (N_j C_j) - \bar{K} (N_j C_j) - \bar{Q} - \frac{\partial}{\partial t} (N_j C_j) \right] N_i dZ = 0 \quad [3.10]$$

Integrating eqn (3.10) will lead to the element equation in matrix form,

$$[K] \{q_c\} + [K_T] \{\dot{q}_c\} = \{Q_c\} \quad [3.11]$$

where $\{q_c\} = \begin{bmatrix} c_1 \\ c_2 \end{bmatrix}$

$$\dot{q}_c = \begin{Bmatrix} \frac{\partial c_1}{\partial t} \\ \frac{\partial c_2}{\partial t} \end{Bmatrix}$$

$$[K] = \int_{z_1}^{z_2} \{ [B]^T D [B] dz + [N]^T v [B] + [N]^T \bar{K} [N] \} dz$$

$$= \begin{bmatrix} \frac{D}{\ell} - \frac{v}{2} + \frac{\bar{K}\ell}{3} & -\frac{D}{\ell} + \frac{v}{2} + \frac{\bar{K}\ell}{6} \\ -\frac{D}{\ell} - \frac{v}{2} + \frac{\bar{K}\ell}{6} & \frac{D}{\ell} + \frac{v}{2} + \frac{\bar{K}\ell}{3} \end{bmatrix}$$

$$[K_T] = \int_{z_1}^{z_2} A [N]^T [N] dz$$

$$= \frac{A\ell}{3} \begin{bmatrix} 1 & \frac{1}{2} \\ \frac{1}{2} & 1 \end{bmatrix}$$

$$Q_c = \int_{z_1}^{z_2} Q [N]^T dz + DN_I \frac{\partial c}{\partial n} \Big|_{z_1}^{z_2}$$

Assembly of the element eqn (3.11) will lead to the global eqn (3.12) which in matrix form is

$$[K] \{r\} + [K_t] \{\dot{r}\} = \{R\} \quad [3.12]$$

Where $[K]$ and $[K_t]$ are the assembled property matrices, $\{R\}$ is the assembled force vector and $\{r\}$ is the assembled nodal concentration.

3.4 Solution in time

There are various time integration schemes available to solve the global eqn (3.12). The selection of time integrator depends on factors desired, such as accuracy, stability and ease of computer implementation. A general β method of time integration scheme is adopted here:

$$\left[\frac{K_t}{\Delta t} + \beta [K]_{t+\Delta t} \right] \{r\}_{t+\Delta t} = \left[\frac{K_t}{\Delta t} - (1 - \beta) [K]_t \right] \{r\}_t + (1 - \beta) \{R\}_t + \beta \{R\}_{t+\Delta t} \quad [3.13]$$

where β ($0 \leq \beta \leq 1$) is a scalar. Table 4 on page 28 gives the various methods available depending on the values of β . The accuracy and stability depends upon the eigen-values of the matrices $[K]$ and $[K_t]$. These matrices are dependent on time step Δt . When Δt exceeds a certain value, the Forward Difference Method becomes unstable. For $\beta = \frac{1}{2}$ or $\beta = \frac{2}{3}$ there will be numerical oscillations when Δt is too large. These methods are unconditionally stable. The Backward Difference Method is less accurate for large Δt . However, this method is unconditionally stable and the calculated values do not oscillate about the correct values.

β	Method
0	Forward difference
$\frac{1}{2}$	Central difference
$\frac{2}{3}$	Galerkin's method
1	Backward difference

Table 4. Time integration methods

3.5 Non Linear Technique

3.5.1 Picard's method

Nonlinear problems are usually solved by taking a series of linear steps. An equilibrium equation written in the form $[K]\{D\} = \{R\}$ is nonlinear when the stiffness matrix $[K]$ is a function of $\{D\}$.

To solve this equation, the first step is to assume a value for $\{D\}$ and calculate $[K]$. The current $[K]$ is used to compute the next $\{D\}$ and the process is repeated until the convergence to the desired solution D_A (Figure 6 on page 30). Usually, the criterion for convergence is chosen as $|D_{i+1} - D_i| \leq \varepsilon D_i$, where i is the number of iteration and ε is the desired accuracy.

3.5.2 Newton - Raphson method

This method is illustrated in Figure 7 on page 31. If there is a solution $D = D^i$ for the equation $f(D) = [K]\{D\} - \{R\} = 0$, the equation can be written using a truncated Taylor series expansion

$$f(D^{i+1}) = f(D^i) + \left(\frac{df}{dD}\right)_i \Delta D^i = 0$$

with $D^{i+1} = D^i + \Delta D^i$.

The improved value of D^{i+1} is obtained by using

$$\Delta D^i = - (K_T^i)^{-1} f^i$$

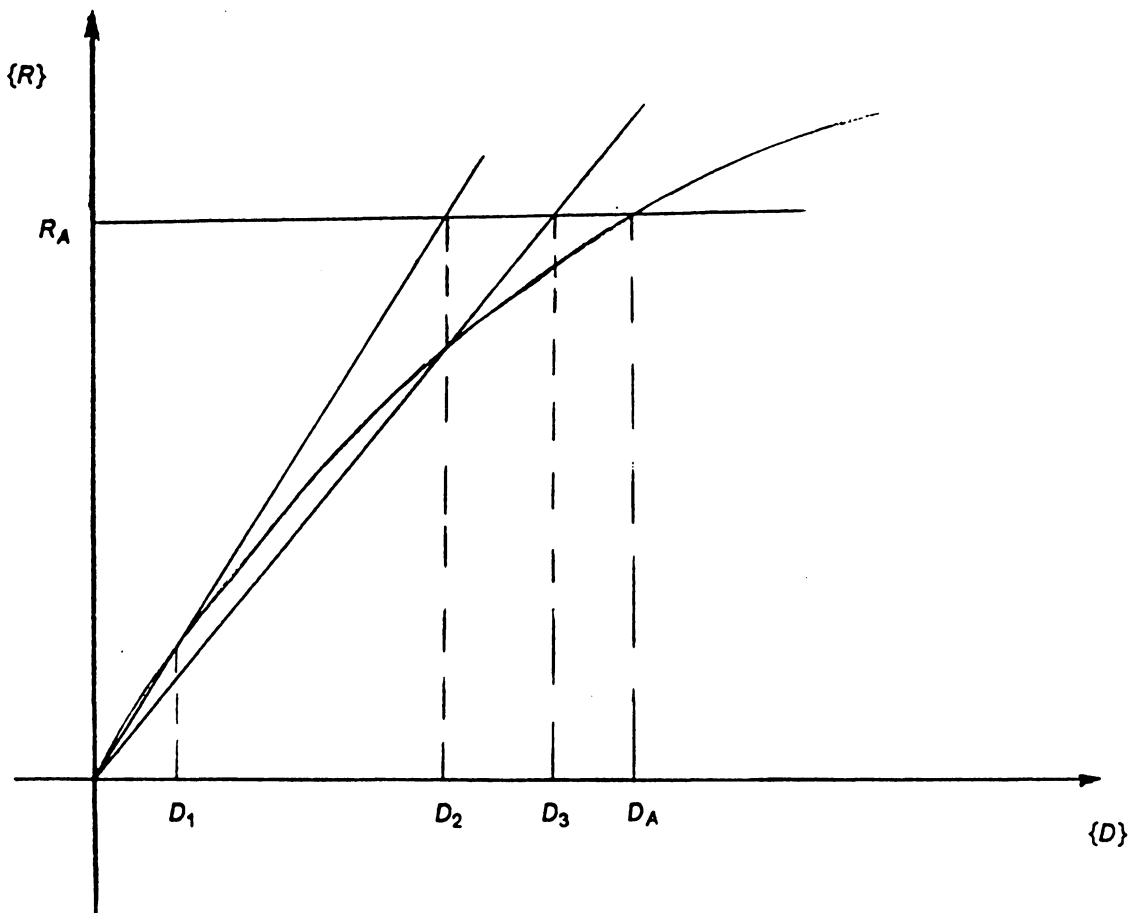


Figure 6. Picard's method

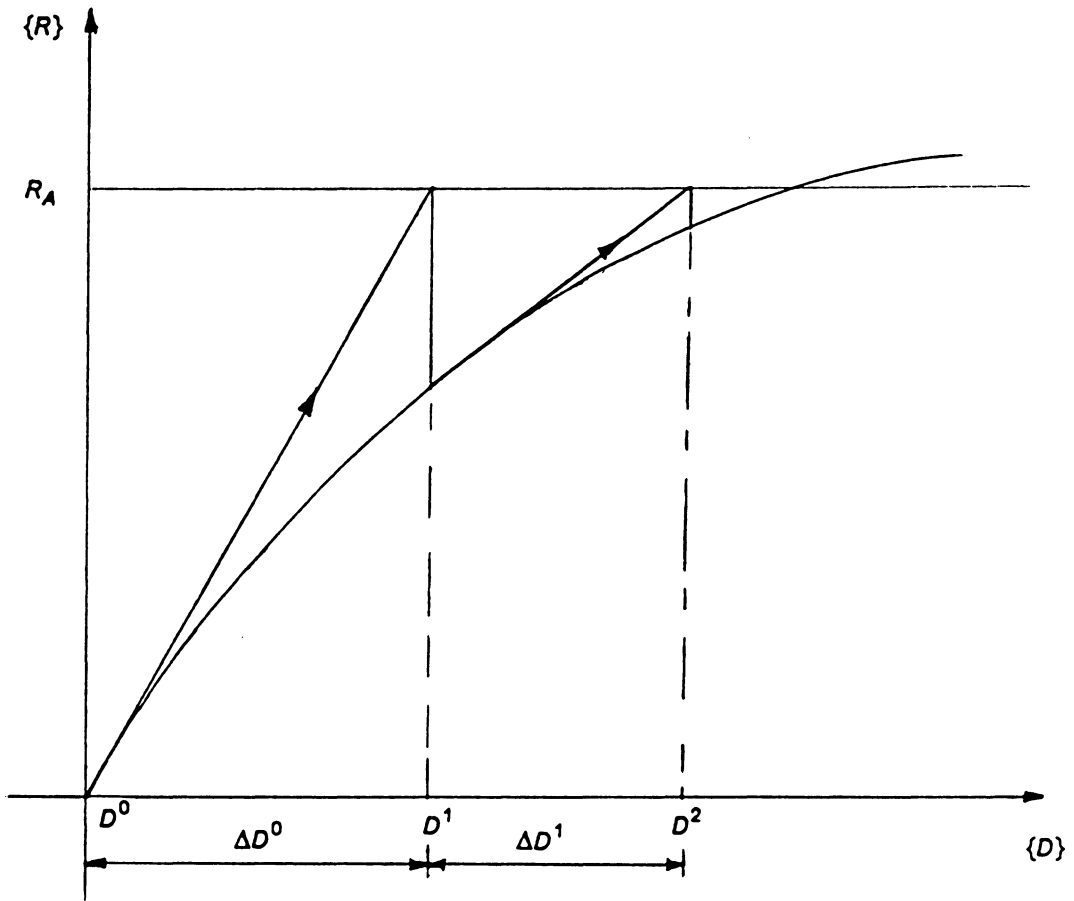


Figure 7. Newton - Raphson method

where (K_T) is the tangential matrix. Near the solution, this method converges, but if the initial assumed value is not close, divergence might occur.

Generally, the Newton-Raphson Method converges faster than the Picard Method. However, to compute the tangent, the derivative of the equation should be taken. This makes the calculation complicated and still does not guarantee convergence. Hence, in this study Picard's Method has been adopted.

In our case, the nonlinearity involved in the governing equation presents an S curve as in Figure 8 on page 33. Therefore, in this program, after each iteration, from the new value of D_2 obtained and the previous value D_1 , the average is taken to get D_3 (i.e., $D'_3 = (D_1 + D_2)/2$), which will be used to update the stiffness matrix $[K]$. This process tends to make the convergence faster. In the present formulation, this technique has been adopted to calculate C_h and k , and to solve Eqn (3.7).

3.6 POLUTE1D

A computer program POLUTE1D has been developed to do the above calculations in the mainframe and personal computer. The program calculates the nodal h using the nonlinear techniques mentioned in the previous section and hence the mean pore velocity. This velocity is substituted in the dispersion equation to obtain the dispersion coefficient. The mass transport equation uses this coefficient and the velocity to compute the nodal concentration at each time step.

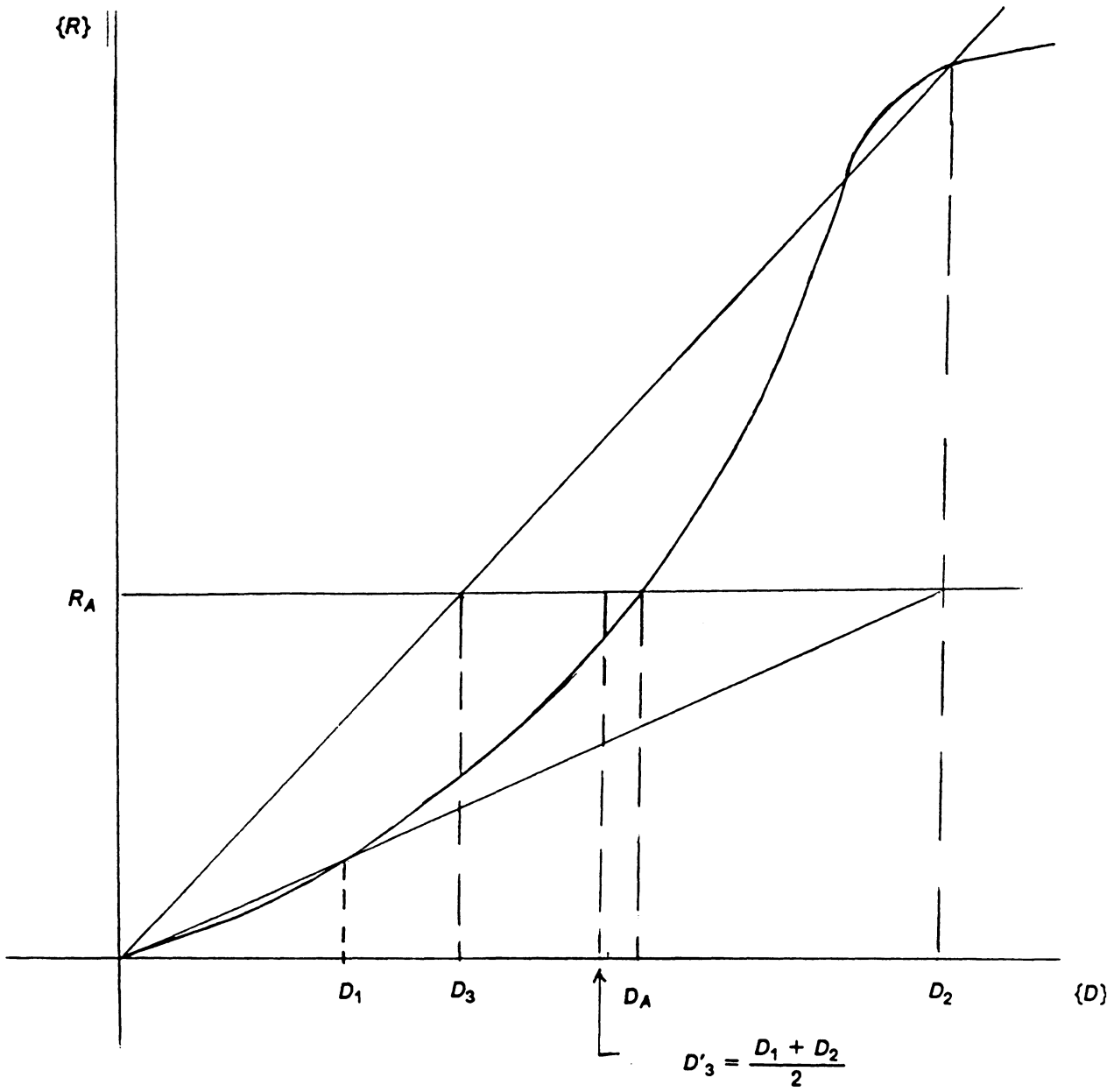


Figure 8. Modified Picard's method

Chapter 4

Parameteric Study

4.1 Introduction

In this chapter, the effects of the various parameters involved in a one-dimensional pollutant transport problem in a porous medium is studied. For this purpose, a typical one-dimensional problem is chosen, as shown in Figure 9 on page 35. A toxic waste material with concentration C_0 is disposed at the top of the lagoon. The water table is located at a depth of H_s feet below the ground. The landfill has a liner thickness of h_t feet. Because of flood conditions, the ponding depth at the top is assumed as h_w feet.

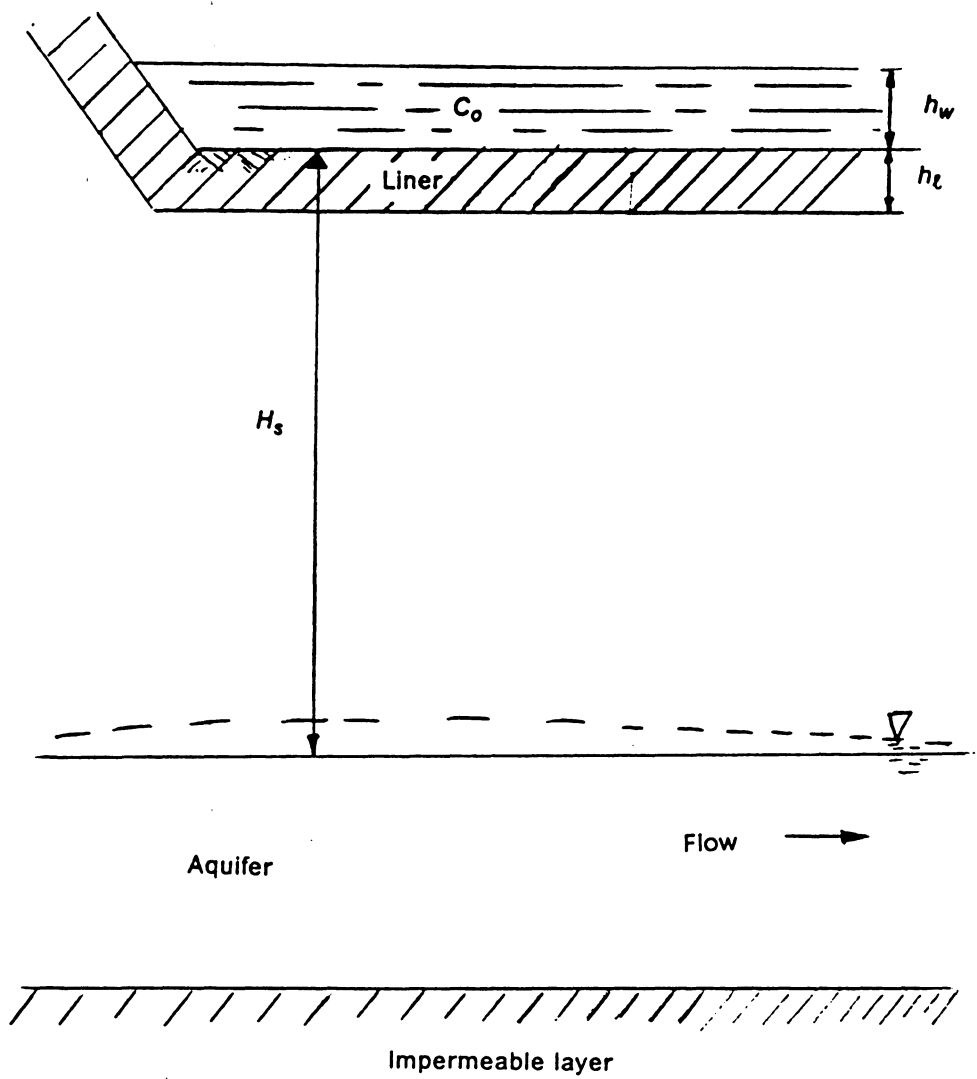


Figure 9. One-dimensional problem

4.2 Parameters

For our study we assume the soil at the location of the landfill as sandy clay loam. The liner material for the landfill is chosen as clay. The representative parameter values for the two materials used in this study is given in Table 5 on page 37. The toxic waste at the site is considered as an inorganic chemical, which is not radioactive or biodegradable. Hence the value of \bar{K} in the mass transport eqn (2.8) may be assumed as zero. Since we are not considering any source or sink in the system, \bar{Q} also becomes zero in eqn (2.8). From Table 3 on page 20 the diffusion coefficient D_0 for the chemical waste is $10^{-3} \text{ ft}^2 \text{ day}^{-1}$. The retardation coefficient R is assumed one.

In our problem we are assuming the total depth H_s as 10 feet. The sandy clay loam overlies an aquifer, which has a very large transmissivity. Due to the presence of the aquifer, there is a mounted water table at the bottom of the soil layer. Hence at the bottom layers soil is saturated and pressure head h may be considered to be zero. The $\theta - h$ distribution for the sandy clay loam and clay is given in Figure 10 on page 38. It was found that a twenty element mesh was adequate for the finite element analysis. Hence in our analysis each element measures 0.5 feet.

For the following analysis unless otherwise stated, the total head for the initial condition is taken as zero, assuming a state of equilibrium. Also the ponding head is kept zero for all the following analysis except for the study, of the effect of the ponding head on the pollutant migration. The datum line is at the water table level. The concentration and the total head at the surface (i.e., at the top node) of the porous medium is kept bounded. If we assume the transmissivity of the aquifer to be very high, the fluctuation in the pressure head h with time, could be neglected for our analysis. Hence at the bottom of the soil layer the total head may be bounded as zero. The concentration at the bottom node is allowed to build up.

Soil	Parameter	Parameter Values
sandy clay loam	α	0.71
	n	1.5
	θ_r	0.1
	θ_s	0.4
	k_s	0.3
clay	α	0.15
	n	1.2
	θ_r	0.15
	θ_s	0.4
	k_s	0.0003 - 0.03

Table 5. Representative values for sandy clay loam and clay (Kool et al., 1986) Units of α in ft^{-1} , k_s in ft day^{-1}

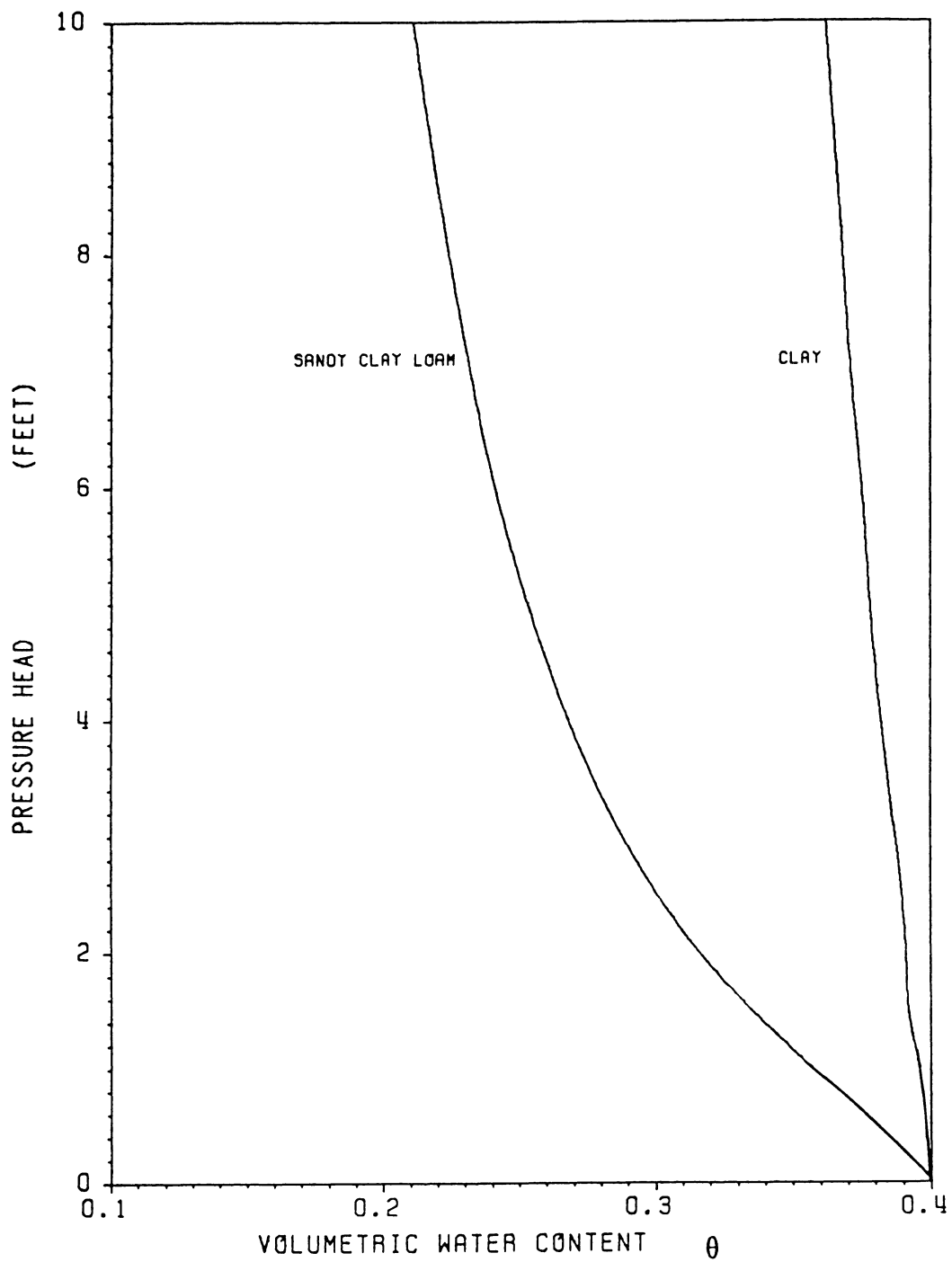


Figure 10. θ - h relationship for sandy clay loam and clay used in the example.

All the analysis in this thesis is done by using the program POLUTE1D. In the following figures the concentration C in the porous domain is given as a ratio $\frac{C}{C_0}$, where C_0 is the concentration introduced at the surface. In our analysis this concentration is assumed to remain constant with time. The effects of the thickness, permeability and dispersivity of the liner, the ponding pressure and the initial condition of the domain on pollutant transport is studied by varying the above factors.

4.3 The effect of liner thickness

In Figure 11 on page 40 the depth vs the concentration ratio for the porous domain is given after the introduction of the contaminant. It takes 340 days for the contaminant ratio to become one at the bottom node, for a no liner condition. The spread of the contaminant, after a one foot liner has been introduced for the landfill is given for time levels 312, 3860 and 42000 days. For this case the liner k_s is taken as $0.0003 \text{ ft day}^{-1}$. For the entire domain to have a concentration of C_0 it takes 115 years with a one foot liner, compared to the 340 days it takes to achieve the same result with a no liner condition. This figure clearly indicates the strong effects of the liner in pollutant spread.

The effect of different liner thicknesses is presented in Figure 12 on page 41. It is a plot of time vs $\frac{C}{C_0}$, where time is on a log scale in the Y axis. The liner k_s is kept constant at $0.0003 \text{ ft day}^{-1}$. The concentration of the pollutant in the landfill is C_0 . The change in concentration at a point A, 10 feet below the surface is plotted, for a no liner condition and after a liner of 1.0 and 1.5 feet has been introduced. This figure shows that the contaminant ratio to become one at point A, it takes approximately 1, 55, and 1180 years for a no liner, 1.0 and 1.5 feet liner conditions respectively. From this figure the remarkable effect of the liner thickness on pollutant transport could be interpreted.

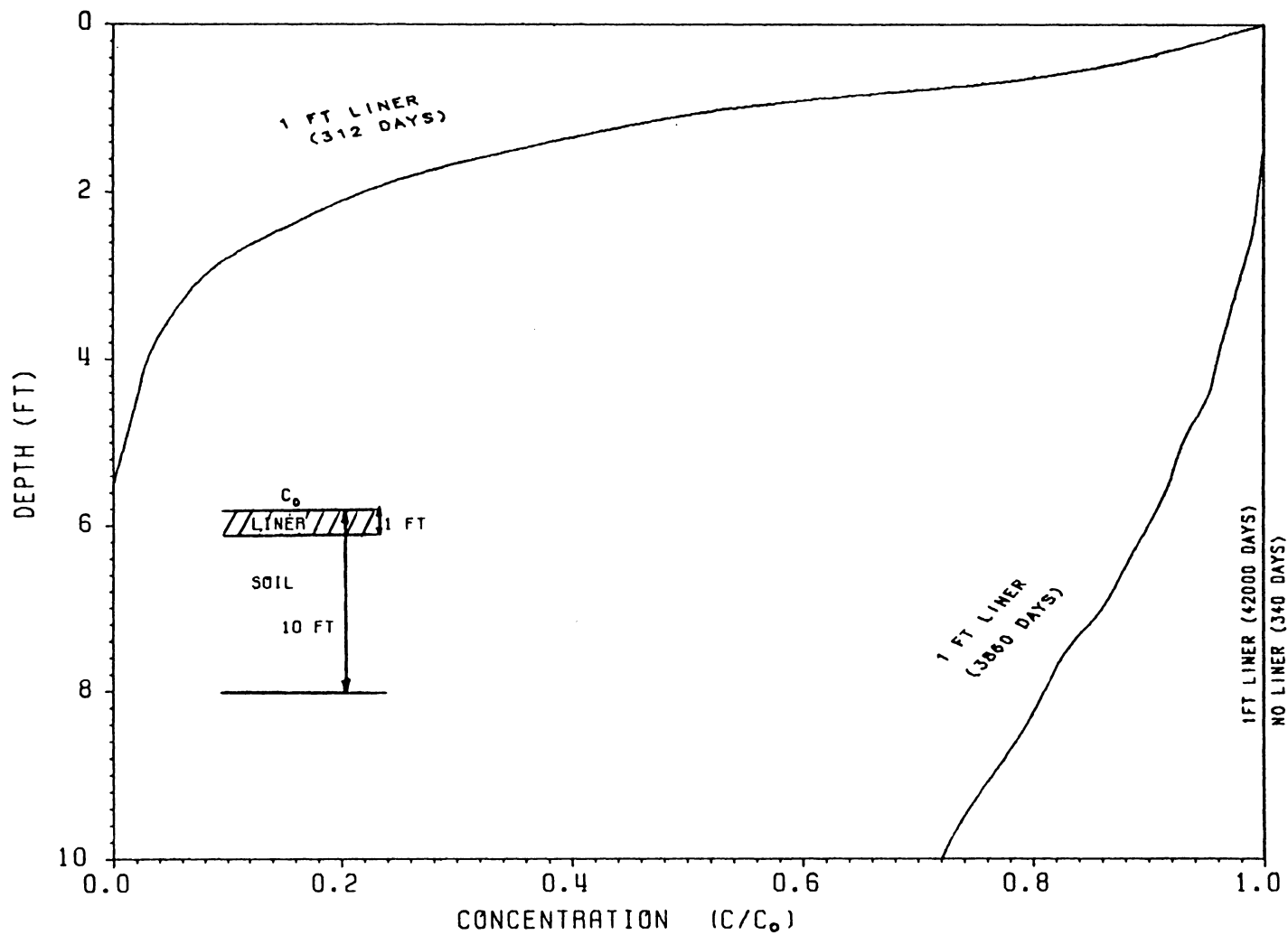


Figure 11. Pollutant spread with time in the porous medium

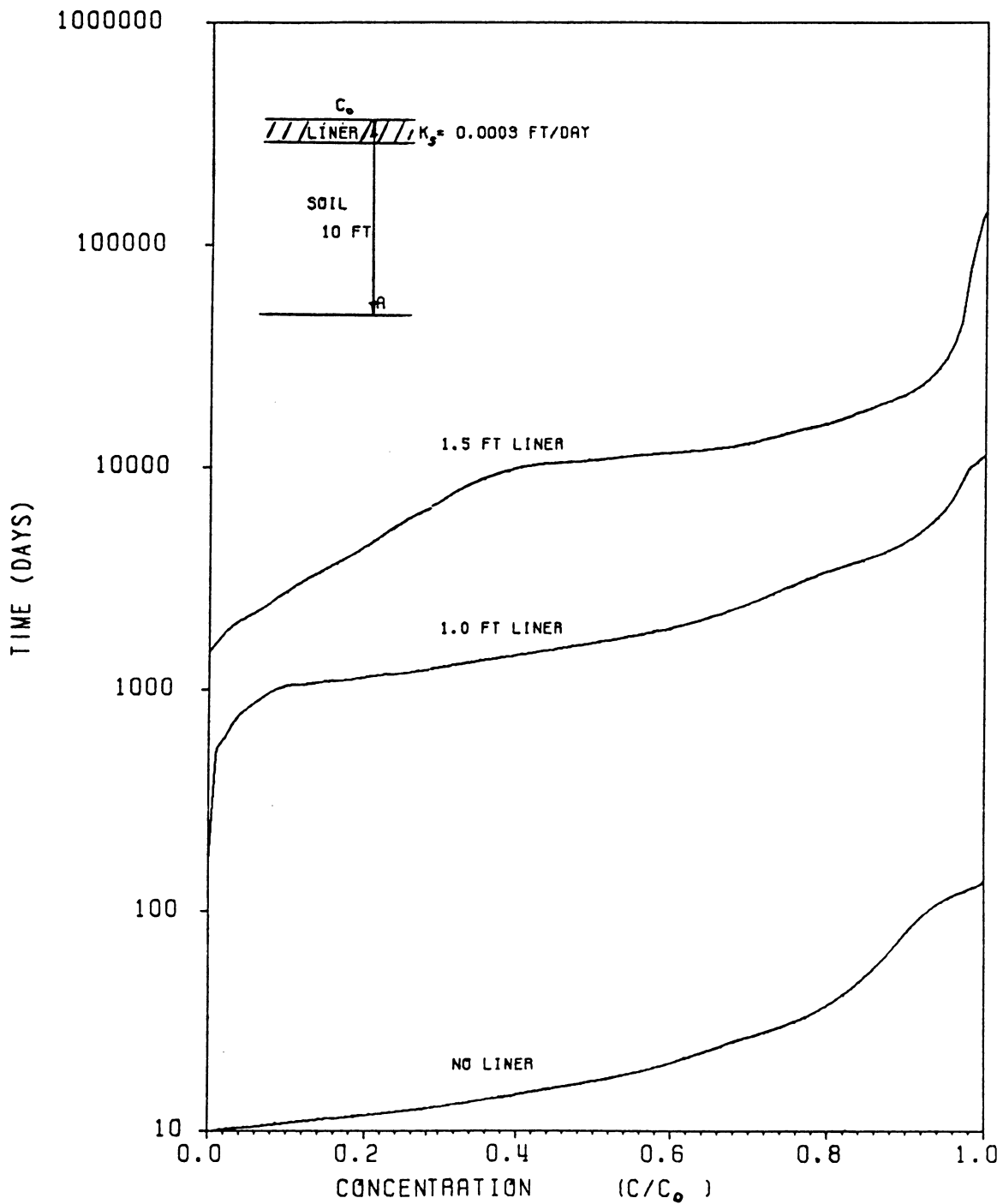


Figure 12. Effect of liner thickness on pollutant transport

4.4 The effect of liner permeability

In Figure 13 on page 43 the liner thickness is kept constant at 1.5 feet and the permeability of the liner is varied from $0.0003 \text{ ft day}^{-1}$ to 0.03 ft day^{-1} . The Y axis is the time in log scale and the X axis is the concentration ratio. The concentration at point A, ten feet below the surface is plotted against time. For a low permeability ($0.0003 \text{ ft day}^{-1}$) liner the concentration at A to become C_0 it takes approximately 1180 years, whereas for a liner with permeability 0.03 ft day^{-1} it takes about 13 years. When the landfill does not have any liner it may be noted from Figure 12 on page 41, for the same conditions it takes only one year for point A to get C_0 concentration. This figure clearly shows the dramatic effect of the permeability.

4.5 The effect of liner dispersivity

Figure 14 on page 44 is the same type of time vs $\frac{C}{C_0}$ graph as explained previously, plotted for the change in concentration at point A, which is ten feet below the surface. The liner thickness and permeability is kept constant at 1.5 feet and $0.0003 \text{ feet day}^{-1}$ respectively. Two curves are plotted for liner dispersivities of 0.078 inches and 1.8 inches. From the curves it could be concluded that the effect of dispersivity of the liner, on pollutant spread is negligible.

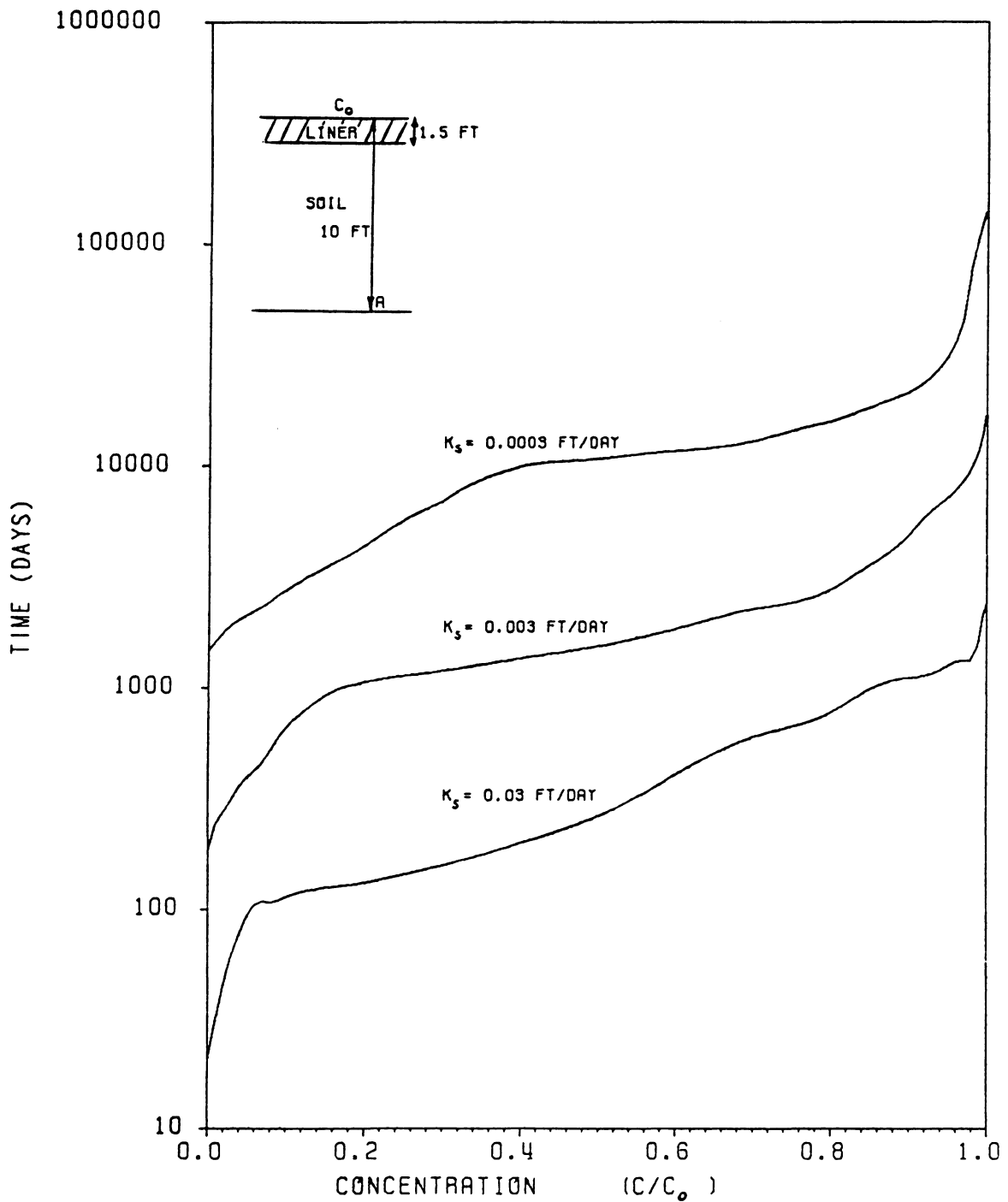


Figure 13. Effect of liner permeability at a point

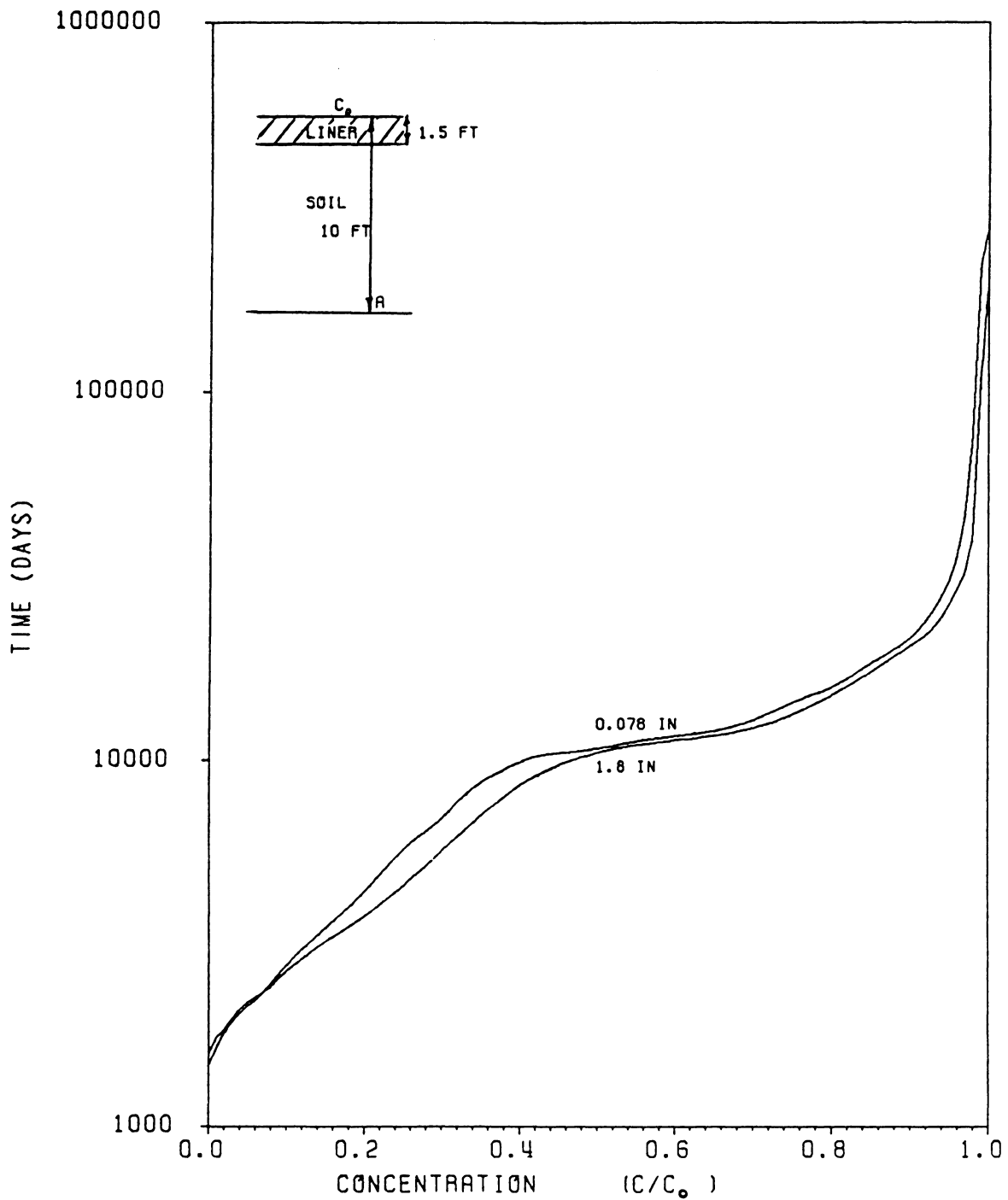


Figure 14. Effect of liner dispersivity at a point

4.6 The effect of ponding depth

In Figure 15 on page 46 the effect of the ponding depth is analysed. For the same initial condition the ponding depth h , is varied from 0 to 3 feet. That is, in this instance the top boundary condition for the total head is changed from 10 to 13 feet. The liner thickness is 1.5 feet and the liner k_s is $0.0003 \text{ ft day}^{-1}$. Again the change in concentration at point A which is 10 feet below the surface is plotted against time. The Y axis has time in log scale. From the curves it could be seen that the effect of the ponding depth is marginal.

4.7 The effect of initial condition

The effect of the initial condition on pollutant transport in the porous medium is shown in Figure 16 on page 47. The total head at the surface for the for the initial condition is taken as -200 feet. This means that the porous domain, is initially in a dry condition. The curves are plotted for conditions of no liner, 1.0 and 1.5 feet liners. These curves are similar to the curves in Figure 12 on page 41, except for the initial condition. However by comparison of Figure 12 on page 41 and Figure 16 on page 47 it could be seen that the curves look almost the same and it may be stated that the initial condition does not affect the pollutant dispersion.

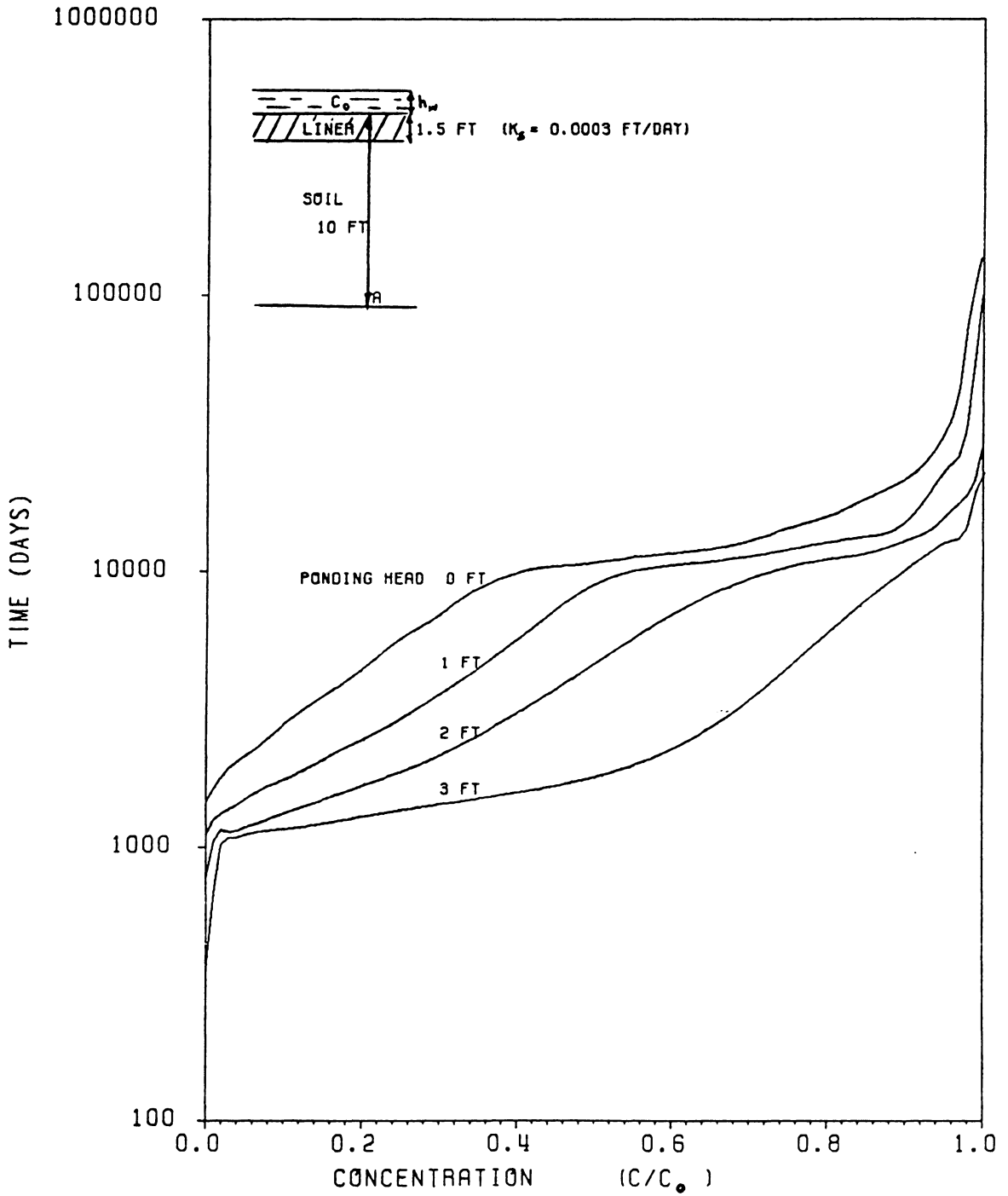


Figure 15. Effect of ponding depth on pollutant transport

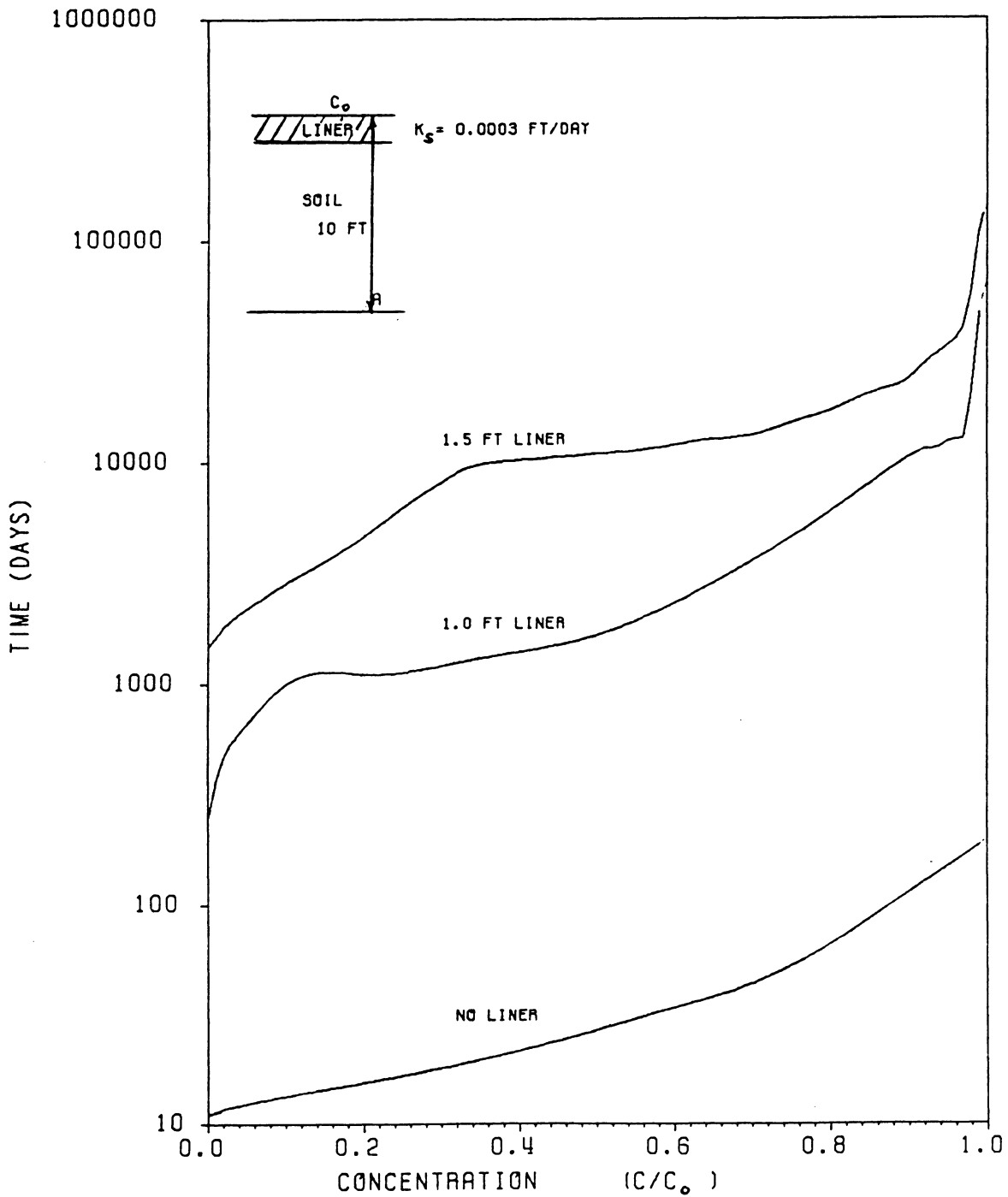


Figure 16. Effect of the initial condition

Chapter 5

Summary and Conclusions

Modeling is probably the most important aspect of solving a subsurface flow problem. In this study a computer program POLUTE1D has been developed based on a one dimensional pollutant transport model. This program has been demonstrated to be a versatile tool in predicting one dimensional pollutant transport in a porous medium.

The model is based on the flow and mass transport equations. These equations depend on the values of C_h and k . C_h is the slope of the θ vs h curve. From the VanGenuchten model k can be calculated. The dispersion coefficient is a function of the velocity. This coefficient is used in the mass transport equation to compute the nodal concentration.

In the preceding analysis the pollutant concentration C_0 at the surface was assumed to remain constant, independent of time. This is a very conservative estimate. Also in the analysis on the effect of the ponding head h_w , again it was assumed that h_w remains constant with time.

For the solution in time, if the time increment for each step is small, the numerical oscillations in the output data may be avoided. That is, the smaller the time increment the more accurate the output becomes. However as the analysis was performed until the entire porous domain reach the same concentration C_0 as in the landfills, the total time involved in the analysis is very large. This precludes the economical use of a constant small time step. Therefore in the present analysis a gradually increasing time step was used to optimise the computer time.

To prevent the pollutant infiltration into the ground from a waste pond an impermeable thick liner should be used. From the plots in the previous chapter, it could be seen that the permeability and the thickness of the liner has a very large effect on the migration of the pollutant than any other factors. The effects due to these factors are almost similar.

The dispersivity of the liner does not have much control over the contaminant spread. Marginal effects were seen due to the changes in the ponding depth and initial condition of the porous domain.

This one dimensional program is applicable only in an extensive waste pond. If the breadth of the dump site is smaller than the length, a two dimensional model should be used. These models are predictive models. However, to establish confidence, the numerical model has to be compared with the field observations. Until such tests are done, this model should be used in field situation with caution.

Bibliography

- Bear, J., "Dynamics of fluids in porous media", Elsevier, New York, 1972.
- Bear, J. and M.Y. Corapcioglu, "Fundamentals of transport phenomena in porous media", Martinus Nijhoff, Dordrecht, 1984.
- Bear, J. and D.K. Todd, "The transition zone between fresh and salt waters in coastal aquifers", University of California, Water Resources Center Contrib., No 29, 1960.
- Brigham, W.E., P.W. Reed and J.N. Dew, "Experiments in mixing during miscible displacement in porous media", Soc. Petrol. Eng. J., 1:1-8, 1961.
- Desai, C.S., "Elementary finite element method", Prentice-Hall Inc., New Jersey, 1979.
- Edwards, M.F. and J.F. Richardson, "Gas dispersion in packed beds", Chem. Eng. Sci 23:109-123, 1968.
- Ghuman, B.S. and S.S. Prihar, "Chloride displacement by water in homogeneous columns of three soils", Soil Sci. Soc. Am. J., 44:17-21, 1980.
- Guymon, G.L., "Mathematical modeling of movement of dissolved constituents in ground water aquifers by the finite element method", Ph.D Dissertation, UCLA, Davis, 1970.
- Harleman, D.R.F., P.F. Mehlhorn and R.R. Rumer, "Dispersion permeability correlation in porous media", J. Hydraul. Div. ASCE 89:67-85.
- Hilby, J.W., "Longitudinal and transverse mixing during single phase flow through granular beds. In interaction between fluids and particles.", Institution of Chem. Eng., London, Symp. Ser No 9, 312-325, 1962.
- Huyakorn, P.S. and G.F. Pinder, "Computational methods in subsurface flow", Academic Press Inc., New York, 1983.
- Kool, J.B., J.C. Parker and M.Th. van Genuchten, "Determining soil hydraulic from one-step outflow experiments by parameter estimation. II Experimental studies", Soil Sci. Soc. Am. J., 1985.

- Kool, J.B. and J.C.Parker, "Development and evaluation of closed form expression for hysteretic soil hydraulic properties", *Water Resources Res.* (in review), 1986.
- Mualem, Y., "A new model for predicting the hydraulic conductivity of unsaturated porous media", *Water Resources Res.*, 12:513-522, 1976.
- Rose, D.S., "Hydrodynamic dispersion in porous materials", *Soil Sci.*, 123:277-283, 1977.
- Rowe, R.K. and J.R.Booker, "1D Pollutant migration in soils of finite depth", *Geotechnical Res. Report GEOT-5-83*, 1984.
- Saffman, P.G., "Dispersion due to molecular diffusion and macroscopic mixing in flow through a network of capillaries", *J. Fluid Mech*, 7:194-208, 1960.
- Taylor, G.I., "Dispersion of solubale matter in solvent flowing slowly through a tube", *Proc. Roy. Soc. A*, No 1137, 219:186-203, 1953.
- Van Genuchten, M.Th., "A closed form equation for predicting the hydraulic conductivity of unsaturated soils", *Soil Sci. Soc. Am. J.*, 44:892-898, 1980.
- Van Genuchten, M.Th., "Calculating the unsaturated hydraulic conductivity with a new closed form analytical model", *Research report 78-WR-08*, Dept. of Civil Eng., Princeton University, Princeton, New Jersey, 1978.
- Zienkiewicz, O.C., "The finite element method", McGraw-Hill, UK, 1977.

The vita has been removed
from the scanned document